01 May 2008

Improved Frequency-Domain Channel Estimation for Fast Time-Varying MIMO-SCFDE Channels

Y. Rosa Zheng
Missouri University of Science and Technology, zhengyr@mst.edu

Jian Zhang

Recommended Citation

Y. R. Zheng and J. Zhang, "Improved Frequency-Domain Channel Estimation for Fast Time-Varying MIMO-SCFDE Channels," *Proceedings of the IEEE International Conference on Communications, 2008. ICC'08*, Institute of Electrical and Electronics Engineers (IEEE), May 2008.
The definitive version is available at https://doi.org/10.1109/ICC.2008.959

This full text paper was peer reviewed at the direction of IEEE Communications Society subject matter experts for publication in the ICC 2008 proceedings.

Improved Frequency-Domain Channel Estimation for Fast Time-Varying MIMO-SCFDE Channels

Yahong Rosa Zheng and Jian Zhang
Department of Electrical & Computer Engineering
Missouri University of Science and Technology, Rolla, MO 65409, USA
Email: zhengyr@mst.edu and jzphd@mst.edu

***Abstract*— A frequency-domain channel estimation method is proposed for time-varying multiple-input multiple output (MIMO) single-carrier frequency-domain equalization (SC-FDE). The proposed method uses frequency-domain interpolation to obtain channel frequency responses of data blocks from estimated responses of two adjacent pilot blocks. It takes the channel temporal-spatial correlation into account to achieve minimum mean squared error (MMSE) estimation, thus improving the accuracy and effectiveness in high Doppler scenarios. The simulation results of the bit error rate (BER) performances show that the proposed method works well for fast time-varying channels with Doppler spread as high as 300 Hz while maintaining over 70% data efficiency.**

I. Introduction

Single-carrier frequency-domain equalization (SC-FDE) has been adopted as the uplink scheme for broadband high speed wireless communications, in contrast to orthogonal frequency division multiplexing (OFDM) for downlink communications. SC-FDE enjoys the same performance and overall computational complexity as OFDM while having less problems with peak-to-average power ratio and less sensitivity to carrier frequency errors [1]. Accurate channel estimation plays an important role in practical SC-FDE systems. The Bit Error Rate (BER) of SC-FDE systems under rapid fading channels can degrade significantly by 3 to 10 dB [2] than those in quasi-static fading channels.

Recently, several studies have been reported in the literature for frequency-domain channel estimation in rapid time-varying channels. A common approach is to employ least mean squares (LMS) or recursive least squares (RLS) adaptive estimation. For example, initial training blocks are employed in [2], [3], [4] for LMS/RLS equalization; unique words are used in each data block in [9] for MIMO (Multi-input Multi-output) RLS estimation algorithm; and pilot symbols in each data block are used to perform structured or unstructured LMS/RLS estimation in [5], [6], [7]. These methods can achieve excellent performance over slow fading channels with maximum Doppler frequency up to several ten Hz. A frequency-domain interpolation method has been proposed in [8] using estimates of two pilot blocks to interpolate the channel frequency response for the data blocks in between. The interpolation utilizes only the individual sub-channel of the two pilot blocks to estimate the corresponding sub-channel of the data blocks thus having very low computational complexity. Excellent performances have been demonstrated for Single-Input Multiple-output (SIMO) channels. No spatial or inter-tap correlation has been taken into account in [8]. In this paper, we extend the frequency-domain interpolation method to MIMO channel estimation. We also consider the spatial correlation among the sub-channels of the receive antennas and the inter-tap correlation of the frequency-selective channel. Simulation results show that including spatial correlation improves estimation accuracy with slightly increased computational complexity. Inter-tap correlation affects the performance slightly with significantly increased computational complexity.

The following notions are used in the paper: lowercase bold fonts represent time-domain vectors or matrices, uppercase bold fonts denote frequency-domain vectors or matrices. The operator $\mathcal{E}$ is the expectation, $j = \sqrt{-1}$, and $\mathbf{I}_m$ is the $m \times m$ identity matrix. Superscripts $(\cdot)^*$, $(\cdot)^{-1}$, $(\cdot)^T$ and $(\cdot)^H$ denote the complex conjugate, inverse, transpose and conjugate transpose respectively.

II. MIMO-SCFDE Transceiver Architecture

Consider a spatial multiplexing MIMO system with n_T transmit antennas and n_R receive antennas. The baseband equivalent system model of the MIMO-SCFDE transceiver is shown in Fig. 1. At the transmitter, the data stream is split into n_T independent branches by a serial-to-parallel (S/P) converter. At each branch, the data stream is partitioned into blocks of N symbols, denoted $\mathbf{x}_t = [x_t(1), \ldots, x_t(n), \ldots, x_t(N)]^T$, for $t = 1, \ldots, n_T$. A length-N_c cyclic prefix (CP) is inserted into each data block, which is a copy of the last N_c symbols of the data block. Several data blocks are grouped into a frame and each frame contains a pilot block, as shown in Fig. 2.

The data stream at each branch is modulated onto a single carrier and transmitted from each antenna across the time-varying and frequency-selective fading channel. At the receive end, the received signals are also corrupted by Additive White Gaussian Noises (AWGN). The signals at each receive branch are processed by a front-end unit consisting of a matched filter, a T_s-spaced sampler, CP remover, and a serial-to-parallel converter. The time-domain baseband signals are converted into frequency-domain by fast Fourier transform (FFT). Then frequency-domain channel estimation, equalization and de-multiplexing are performed, followed by inverse fast Fourier transform (IFFT) to convert the frequency-domain signal to the time-domain signal. Finally, symbol detection is made based on the time-domain signals then a parallel-to-serial (P/S) converter outputs the estimated data sequence serially.

The time-domain MIMO system can be expressed by the baseband equivalent model as

$$\mathbf{y} = \mathbf{g}\mathbf{x} + \mathbf{v} \tag{1}$$

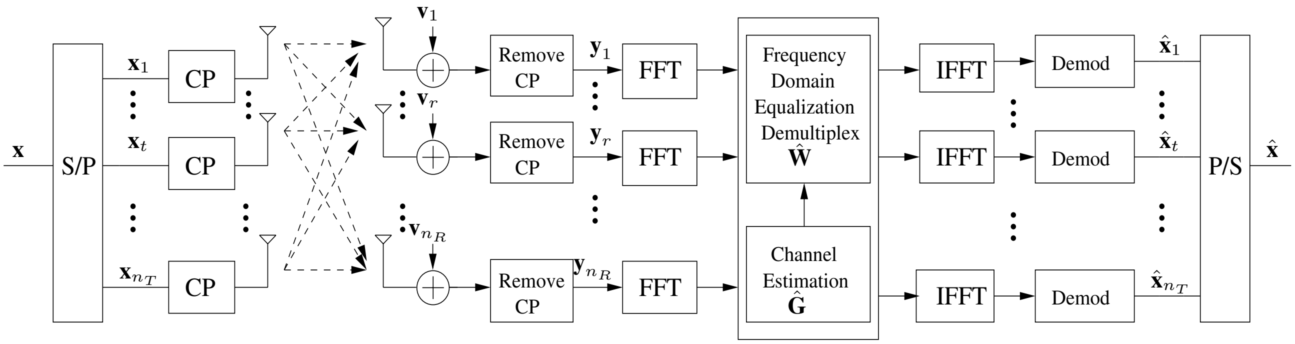

Fig. 1. MIMO-SCFDE system architecture with spatial multiplexing, where n_T and n_R are the number of transmit and receive antennas, respectively.

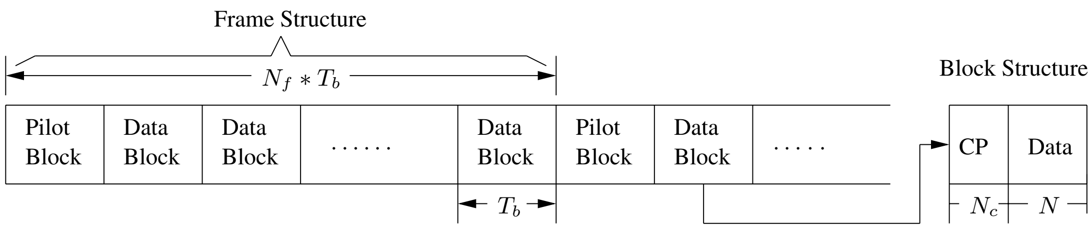

Fig. 2. The frame structure for MIMO-SCFDE, where the period of one block is $T_b = (N + N_c)T_s$ and the frame duration is $T_f = N_f(N + N_c)T_s$, where T_s is the symbol period, and N_f is the number of blocks per frame.

where the concatenated input and noise vectors are $\mathbf{x} = [\mathbf{x}_1^T,\ \mathbf{x}_2^T,\ \ldots,\ \mathbf{x}_{n_T}^T]^T$ and $\mathbf{v} = [\mathbf{v}_1^T,\ \ldots,\ \mathbf{v}_{n_R}^T]^T$, respectively. The output vector $\mathbf{y} = [\mathbf{y}_1^T,\ \mathbf{y}_2^T,\ \ldots,\ \mathbf{y}_{n_R}^T]^T$ with

$$\mathbf{y}_r = \sum_{r=1}^{n_T} \mathbf{g}_{r,t}\mathbf{x}_t + \mathbf{v}_r,$$

and the channel matrix $\mathbf{g} = \{\mathbf{g}_{r,t}\}$ is an $(Nn_R) \times (Nn_T)$ matrix whose (r,t)-th sub-channel impulse response $\mathbf{g}_{r,t}$ can be expressed as an $N \times N$ circulant matrix

$$\mathbf{g}_{r,t} = \begin{bmatrix} g_{r,t}(1) & 0 & \ldots & g_{r,t}(L) & \ldots & g_{r,t}(2) \\ g_{r,t}(2) & g_{r,t}(1) & \ddots & \ddots & \ddots & \vdots \\ \vdots & \ddots & \ddots & \ddots & \ddots & g_{r,t}(L) \\ g_{r,t}(L) & \ddots & g_{r,t}(1) & 0 & \ddots & 0 \\ 0 & g_{r,t}(L) & \ddots & \ddots & \ddots & \ddots \\ \vdots & \ddots & \ddots & \ddots & \ddots & 0 \\ 0 & \ldots & g_{r,t}(L) & \ldots & \ldots & g_{r,t}(1) \end{bmatrix} \quad (2)$$

where L is the length of the channel response and $g_{r,t}$ denotes the impulse response between the t-th transmit antenna and the r-th receive antenna. Note that, in a fast time-varying fading channel, the channel response may vary within one block duration. The circulant matrix model is a valid assumption only when the block duration T_b is smaller than the channel coherence time.

The frequency-domain channel model is obtained by taking Discrete Fourier Transform (DFT) on both sides of (1). Define $\mathbf{B}_K = \mathbf{I}_K \otimes \mathbf{F}_N$, where $\otimes$ denotes the Kronecker product and $\mathbf{F}_N$ is the normalized DFT matrix of size $N \times N$. The (k,n)-th element of $\mathbf{F}_N$ is given by $\frac{1}{\sqrt{N}} \exp\left(\frac{-j2\pi(k-1)(n-1)}{N}\right)$, for $k,\ n = 1,\ 2,\ \ldots,\ N$. Using the property $\mathbf{B}_{n_T}^H \mathbf{B}_{n_T} = \mathbf{I}_{Nn_T}$, we obtain the frequency-domain representation of the MIMO channel as

$$\begin{aligned} \mathbf{Y} = \mathbf{B}_{n_R}\mathbf{y} &= \mathbf{B}_{n_R}\mathbf{g}\mathbf{x} + \mathbf{B}_{n_R}\mathbf{v} \\ &= \mathbf{B}_{n_R}\mathbf{g}\mathbf{B}_{n_T}^H \mathbf{B}_{n_T}\mathbf{x} + \mathbf{B}_{n_R}\mathbf{v} \\ &= \mathbf{G}\mathbf{X} + \mathbf{V} \end{aligned} \quad (3)$$

where the channel frequency response matrix $\mathbf{G}$ is defined by

$$\mathbf{G} = \mathbf{B}_{n_R}\mathbf{g}\mathbf{B}_{n_T}^H = \begin{bmatrix} \mathbf{G}_{1,1} & \ldots & \mathbf{G}_{1,n_T} \\ \vdots & \ddots & \vdots \\ \mathbf{G}_{n_R,1} & \ldots & \mathbf{G}_{n_R,n_T} \end{bmatrix} \quad (4)$$

and $\mathbf{G}_{r,t} = \mathbf{F}_N \mathbf{g}_{r,t} \mathbf{F}_N^H$. Since $\mathbf{g}_{r,t}$ is a circulant matrix, the corresponding frequency response $\mathbf{G}_{r,t}$ will be a diagonal matrix whose inverse is easy to compute. However, the overall channel matrix $\mathbf{G}$ is not diagonal, which does not lead to computational savings in the present form. To take the advantage of the diagonal property along the frequency bins, re-arrange the input and output vectors by each frequency bin

$$\mathbf{X} = [\mathbf{X}^T(1),\ \ldots,\ \mathbf{X}^T(k),\ \ldots,\ \mathbf{X}^T(N)]^T,$$

$$\mathbf{Y} = [\mathbf{Y}^T(1),\ \ldots,\ \mathbf{Y}^T(k),\ \ldots,\ \mathbf{Y}^T(N)]^T$$

where $\mathbf{X}(k) = [X_1(k),\ \ldots, X_t(k),\ \ldots,\ X_{n_T}(k)]^T$ and $\mathbf{Y}(k) = [Y_1(k),\ \ldots, Y_r(k),\ \ldots,\ Y_{n_R}(k)]^T$. Similarly, the channel matrix for the k-th frequency bin is

$$\mathbf{G}(k) = \begin{bmatrix} G_{1,1}(k) & \ldots & G_{1,n_T}(k) \\ \vdots & \ddots & \vdots \\ G_{n_R,1}(k) & \ldots & G_{n_R,n_T}(k) \end{bmatrix} \quad (5)$$

The channel matrix $\mathbf{G}$ is converted into a block diagonal matrix consisting of N smaller matrices $\mathbf{G}(k)$, *i.e.*, $\mathbf{G} = \text{diag}[\mathbf{G}(k)]$. The channel model for each frequency bin is then defined as

$$\mathbf{Y}(k) = \mathbf{G}(k)\mathbf{X}(k) + \mathbf{V}(k), \quad k = 1, \ \ldots, \ N \tag{6}$$

The frequency domain channel estimation and equalization can be performed separately for each k, thus reducing the computational complexity.

III. The Proposed Frequency-Domain Channel Estimation Method

A. Channel Estimation for Pilot Blocks

Channel estimation for pilot blocks relies on careful design of pilot sequences. First, the orthogonality of the pilot sequences are needed to separate the responses of multiple sub-channels at each receive antenna. Second, pilot sequences having constant amplitude over all frequency bins are desirable to avoid noise enhancement. The pilot design proposed in [4] satisfies both requirements. We adopt this pilot design and summarize the channel estimation procedures here.

Step 1. Choose a length-(N/n_T) Chu sequence [11] and duplicate the time-domain Chu sequence for n_T times to yield a length-N training sequence for the first transmit antenna. Denote the training sequence as $\mathbf{p}_1 = [\mathbf{c}, \ \ldots, \ \mathbf{c}]_{1\times N}$, where $\mathbf{c}$ denotes the length-(N/n_T) Chu sequence. The spectrum of the pilot sequence exhibit periodic peaks with $(n_T - 1)$ zeros in between. Construct the pilot sequence for the r-th transmit antenna by rotating $\mathbf{p}_1$ in frequency domain yielding orthogonal pilot sequences.

Step 2. Using the orthogonality property, the channel response at frequency bins $\Psi_t = \{t, \ t+n_T, \ \ldots, \ N-n_T+t\}$ are estimated by $\tilde{G}_{r,t}(k) = \frac{Y_r(k)}{P_t(k)} = G_{r,t}(k) + \frac{V_r(k)}{P_t(k)}$.

Step 3. Multiply a scalar factor n_T with the initial estimation and transform the result into time domain estimate $\tilde{\mathbf{g}}_{r,t}$ by IFFT. Then window $\tilde{\mathbf{g}}_{r,t}$ to remove taps at $n = L+1, \ \ldots, \ N/n_T$. This technique can reduce estimation noise and it was originally proposed for OFDM systems [10].

Step 4. Convert the windowed impulse response into frequency domain. This will provide estimation of frequency response for all frequency bins which can be expressed as

$$\hat{\mathbf{G}}_{r,t} = \mathbf{G}_{r,t} + \hat{\mathbf{V}}_t = \mathbf{F}_N\mathbf{U}\tilde{\mathbf{g}}_{r,t} \tag{7}$$

where $\hat{\mathbf{V}}_t$ is the estimated noise vector and $\mathbf{U}$ is a diagonal windowing matrix whose first L diagonal elements are ones and others are zeros.

B. The New Interpolation Method for Data Block Channel Estimation

The proposed frequency-domain interpolation method utilizes two adjacent pilot blocks to estimate the channel responses of data blocks. Let superscript m be the block index. Let $\hat{G}^1_{r,t}(k)$ and $\hat{G}^{N_f+1}_{r,t}(k)$ be the estimated channel responses of the pilot blocks of the current and next frame, respectively, both corresponding to the k-th frequency bin and the (r,t)-th sub-channel. To consider the spatial correlation among receive antennas in the interpolation method, we define a column vector different from that in [8] as

$$\hat{\mathbf{Z}}_t(k) = \left[\hat{G}^1_{1,t}(k)\ldots\hat{G}^1_{n_R,t}(k) \ \ \hat{G}^{N_f+1}_{1,t}(k) \ \ldots\hat{G}^{N_f+1}_{n_R,t}(k)\right]^T \tag{8}$$

and denote $\mathbf{C}^m_{r,t}(k)$ the corresponding interpolation row vector for the m-th data block in the current frame. The channel response of the data block is given by

$$\hat{G}^m_{r,t}(k) = \mathbf{C}^m_{r,t}(k)\hat{\mathbf{Z}}_t(k), \ m = 2,\ldots,N_f, k = 1,\ldots,N. \tag{9}$$

Then the mean squared estimation error is determined by

$$\epsilon^m_{r,t}(k) = \mathcal{E}\left\{|e^m_{r,t}(k)|^2\right\} = \mathcal{E}\left\{|G^m_{r,t}(k) - \hat{G}^m_{r,t}(k)|^2\right\} \tag{10}$$

The interpolation vector $\mathbf{C}^m_{r,t}(k)$ can be solved by minimizing the mean squared error. Taking derivative of (10) with respect to $\mathbf{C}^m_{r,t}(k)$, we obtain the optimal solution as

$$\mathbf{C}^m_{r,t}(k) = \mathbf{A}\mathbf{R}^{-1} \tag{11}$$

$$\mathbf{A} = \mathcal{E}\left[G^m_{r,t}(k)\hat{\mathbf{Z}}^H_t(k)\right] = [A_1 \ \ldots \ A_{(2n_R)}], \tag{12}$$

$$A_i = \mathcal{E}\left\{G^m_{r,t}(k)(\hat{G}^1_{i,t}(k))^*\right\},$$

$$A_{i+n_R} = \mathcal{E}\left\{G^m_{r,t}(k)(\hat{G}^{N_f+1}_{i,t}(k))^*\right\},$$

$$\mathbf{R} = \mathcal{E}\left[\hat{\mathbf{Z}}_t(k)\hat{\mathbf{Z}}^H_t(k)\right] = \{R_{i,q}\}_{(2n_R)\times(2n_R)}, \tag{13}$$

$$R_{i,q} = \mathcal{E}\left\{\hat{G}^1_{i,t}(k)(\hat{G}^1_{q,t}(k))^*\right\}$$

$$R_{i+n_R,q} = R^*_{q,i+n_R} = \mathcal{E}\left\{\hat{G}^{N_f+1}_{i,t}(k)(\hat{G}^1_{q,t}(k))^*\right\}$$

$$R_{i+n_R,q+n_R} = \mathcal{E}\left\{\hat{G}^{N_f+1}_{i,t}(k)(\hat{G}^{N_f+1}_{q,t}(k))^*\right\}$$

for $i, q = 1,\ldots,n_R$. Here we drop the subscripts and superscripts in (12) and (13) for notation convenience. It is clear that the interpolation vector only depends on the second-order statistics of the channel rather than the instantaneous channel coefficients. For many practical fading channels, the second-order statistics may remain stationary for fixed Doppler frequencies and antenna settings. This is of great advantage because the interpolation vectors can be obtained through off-line training for each base station sector. Some statistic fading models, such as isotropic or non-isotropic scattering, Rayleigh/Ricean/Nakagami models, may also be used to compute the interpolation vectors for different scenarios. The computed interpolation vectors can then be selected and used directly for channel estimation of the data blocks in (9). This leads to great computational savings in real-time processing. An example of isotropic scattering Rayleigh fading channel is given in Section IV.

C. MMSE Channel Equalization

With the estimated channel responses, the frequency-domain MMSE equalizer is determined as

$$\hat{\mathbf{X}}(k) = \sigma^2_x\hat{\mathbf{G}}^H(k)[\sigma^2_x\hat{\mathbf{G}}(k)\hat{\mathbf{G}}^H(k) + \mathbf{\Sigma} + \varepsilon\mathbf{I}_{n_R}]^{-1}\mathbf{Y}(k) \tag{14}$$

where $\hat{\mathbf{G}}(k)$ is the estimated channel response at the k-th frequency bin, $\mathbf{\Sigma} = \text{diag}(\hat{\sigma}^2_1,\ldots,\hat{\sigma}^2_{n_R})$ is the estimated noise variance matrix [4], [8], σ^2_x is the signal power, and ε is the minimum mean squared error of channel estimation.

IV. Simulation Experiments

We use the commonly accepted wide-sense-stationary uncorrelated scattering (WSSUS) Rayleigh fading channel to demonstrate the performance of the proposed method. The interpolation vectors for this type of channel have a closed form solution due to the decomposition property of triply-selective channels [12]. The elements in (12) and (13) are determined as

$$\begin{aligned} A_i &= J_0(\omega_d(m-1)T_b)\Phi^{Rx}_{r,i} \quad (15)\\ A_{i+n_R} &= J_0(\omega_d(N_f-m+1)T_b)\Phi^{Rx}_{r,i}\\ R_{i,q} &= R_{i+n_R,q+n_R} = \Phi^{Rx}_{i,q} f_{gg}(k) + \frac{L}{N}\mu_{i,q} \quad (16)\\ R_{i+n_R,q} &= J_0(\omega_d N_f T_b)\Phi^{Rx}_{i,q} f_{gg}(k) \end{aligned}$$

where $J_0(\cdot)$ is the zero-order Bessel function of the first kind, $\omega_d = 2\pi f_d$ with f_d being the maximum Doppler frequency, $\Phi^{Rx}_{i,q}$ is the spatial correlation coefficient between the i,q-th sub-channel and it normally does not change much with time. The noise correlation $\mu_{i,q} = \sigma_i^2$ for $i = q$ and zero for $i \neq q$. The Fourier transform of the inter-tap correlation is defined as

$$f_{gg}(k) = \sum_{l_1=1}^{L}\sum_{l_2=1}^{L} \Phi^{Tap}_{l_1,l_2} \exp\left(\frac{-j2\pi(l_1-l_2)(k-1)}{N}\right) \quad (17)$$

with $\Phi^{Tap}_{l_1,l_2}$ being the inter-tap correlation between the l_1-th and l_2-th taps of the fading channel. The inter-tap correlation may change slightly faster than the spatial correlation, requiring more frequent adjustment. The derivation of (15) is omitted here due to the page limit.

As a numerical example, a 60-tap frequency-selective Rayleigh fading channel was simulated using the triply-selective fading model [12]. Although the frequency-domain equalizer assumes that channel coefficients are time-invariant within a data block, the simulated channel coefficients change with time especially when the maximum Doppler frequency increases. The power delay profile of the channel was chosen such that the average power of the first 20 taps ramps up linearly and the last 40 taps ramps down linearly. The total average power of the fading channel was normalized to unit. The length of the data block and CP were selected as $N = 256$ and $N_c = 64$, respectively. The symbol duration was set as $T_s = 0.25\mu s$. The overall data efficiency was 72% — similar to other channel estimation methods.

The estimated channel frequency responses (CFR) are shown in Fig. 3(a) and Fig. 3(b) for a pilot block and a data block, respectively. The maximum Doppler spread f_d was 20 Hz. The mean squared error (MSE) of the new channel estimation method approached 10^{-3} when SNR = 20 dB.

The proposed channel estimation method was applied to various MIMO SCFDE and different modulation schemes. The bit error rate (BER) performances under spatially uncorrelated and inter-tap independent channels are shown in Fig. 4. At $f_d = 20$ Hz, the proposed channel estimation method requires approximately 2 dB more SNR to achieve 10^{-3} BER than that of the perfectly-known channel; while the RLS adaptive channel estimation algorithm requires at least 4 dB more SNR to achieve the same performance, as seen in Fig. 4(a). When the channel changes faster, the performance degrades with the increase of f_d, as shown in Fig. 4(b). Nevertheless, acceptable performances can still be achieved when $f_d = 200$ Hz, which is better than those of the existing methods. Further increase of f_d leads to a smaller coherent time than the duration between pilot blocks and data blocks thus resulting in reduced BER performance.

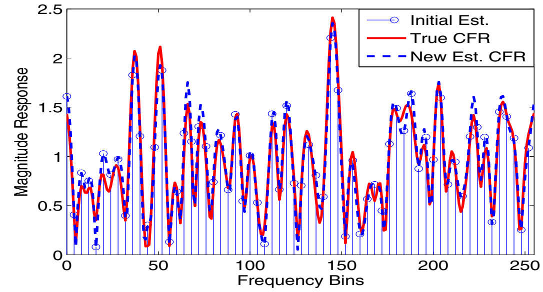

(a) Pilot Block sub-channel $\mathbf{G}_{1,1}$

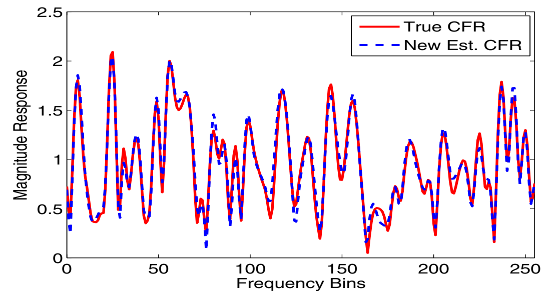

(b) Data Block sub-channel $\mathbf{G}_{2,1}$

Fig. 3. Channel Estimation for 4×4 MIMO channels. SNR=10 dB, $f_d = 20$ Hz, channel length $L = 60T_s$, $T_s = 0.25\mu s$. Block length $N = 256$, CP length $N_c = 64$, frame length $N_f = 10$.

When channel exhibits spatial correlation as well as inter-tap correlation, the proposed method considered spatial correlation and achieved better BER performance than the scheme in [8], as shown in Fig. 5. The spatial correlation among different receive antennas were between -0.2 and 0.5. If channel estimation ignores the correlation, the resulting BER performance is similar to that of Fig. 4. When considering the correlation, higher estimation accuracy was achieved. The BER performances in low Doppler channels were slightly better than that of [8] for both 4×4 and 4×8 systems, as shown in Fig.5(a). In high Doppler channels ($f_d = 300$ Hz), the new method achieved significantly better BER performance than that of [8], as shown in Fig. 5(b).

V. Conclusion

We have presented an improved channel estimation algorithm for MIMO SCFDE using frequency-domain interpolation approach. The improved method takes advantage of the temporal and spatial correlation of the MIMO fading channel to estimate the changes of the channel response of data blocks

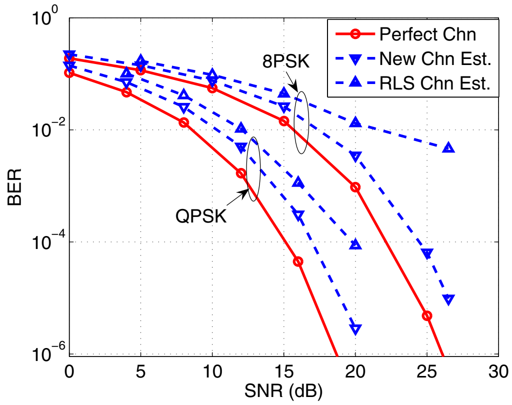

(a) $f_d = 20$ Hz with different modulation

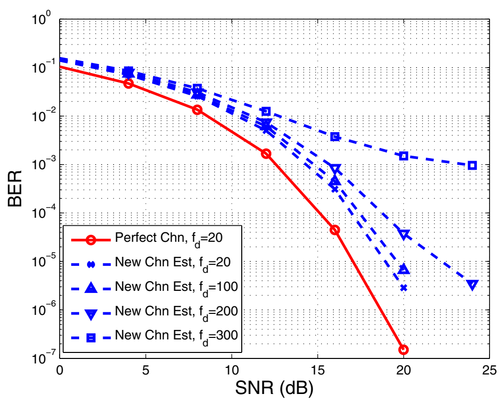

(b) QPSK modulation with different f_d

Fig. 4. BER performances of 4×4 MIMO FDE using the new channel estimation. The fading channel has no inter-tap correlation nor spatial correlation. Other parameters of the channel are the same as those in Fig. 3.

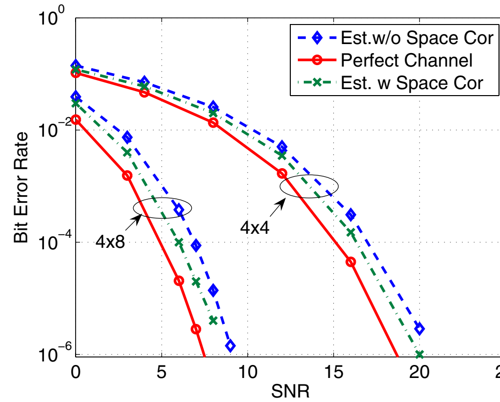

(a) $f_d = 20$ Hz in 4×4 and 4×8 MIMO

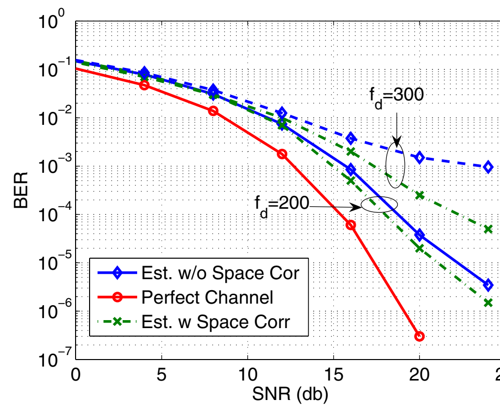

(b) Channel Est. with or w/o spatial correlation

Fig. 5. BER performances of MIMO FDE in triply-selective fading channels. The channel estimation method takes spatial/inter-tap correlation into account and achieves better performance. QPSK modulation was used in all cases.

thus achieving better estimation accuracy. The interpolation vector only depends on the second-order statistics of the fading channels and may be computed through off-line training or statistical channel models. Computer simulation results have shown that the proposed method performs very well in fast time-varying channels with Doppler shifts up to 300 Hz.

VI. Acknowledgement

This work is supported by Office of Naval Research under grant N00014-07-1-0219 and University of Missouri Research Board fund no. 2771.

References

[1] D. Falconer, S. L. Ariyavisitakul, A. Benyamin-Seeyar, and B. Eidson, "Frequency domain equalization for single-carrier broadband wireless systems," *IEEE Commun. Mag.*, vol. 40, no. 4, pp. 58-66, Apr. 2002.

[2] M. V. Clark,"Adaptive frequency-domain equalization and diversity combining for broadband wireless communications," *IEEE J. Select. Areas Commun.*, vol. 16, no. 8, pp. 1385-1395, Oct. 1998.

[3] J. Coon, S. Armour, M. Beach, and J. McGeehan, "Adaptive frequency-domain equalization for single carrier multiple-input multiple-output wireless transmissions," *IEEE Trans. Signal Processing*, vol. 53, no. 8, pp. 3247-3256, Aug. 2005.

[4] J. Siew, J. Coon, R. J. Piechocki, A. Dowler, A. Nix, M. Beach, S. Armour, and J. McGeehan, "A channel estimation algorithm for MIMO-SCFDE," *IEEE Commun. Lett.*, vol. 8, no. 9, pp. 555-557, Sep 2004.

[5] Y. Zhu and K. B. Letaief, "Single-carrier frequency-domain equalization with noise prediction for MIMO systems," *IEEE Trans. Commun.*, vol. 55, no. 5, pp. 1063-1076, May 2007.

[6] M. Morelli, L. Sanguinetti, and U. Mengali, "Channel estimation for adaptive frequency-domain equalization," *IEEE Trans. Wireless Commun.*, vol.4, pp.2508-2518, Sept. 2005.

[7] S. Ahmed, M. Sellathurai, S. Lambotharan, and J. A. Chambers, "Low-complexity iterative method of equalization for single carrier with cyclic prefix in doubly selective channels," *IEEE Sig. Proc. Lett.*, vol.13, pp.5-8, Jan. 2006.

[8] Y. R. Zheng and C. Xiao,"Frequency-domain channel estimation and equalization for broadband wireless communications," *Proc. ICC*, Glasgow, Scotland, June, 2007.

[9] J. Coon, M. Sandell, M. Beach, and J. McGreehan, "Channel and noise variance estimation and tracking algorithms for unique-word based single-carrier systems," *IEEE Trans. Wireless Commun.*, vol. 5, pp. 1488-1496, June 2006.

[10] Ye Li, L. J. Cimini, and N. R. Sollenberger, "Robust channel estimation for OFDM systems with rapid dispersive fading channels," *IEEE Trans.Commnu.*, vol. 46, pp. 902-915, July 1998.

[11] D. C. Chu,"Polyphase codes with good periodic correlation properties,"*IEEE Trans. Inform. Theory*, vol. IT-18, pp. 531-532, July 1972.

[12] C. Xiao, J. Wu, S.-Y. Leong, Y. R. Zheng, and K. B. Letaief, "A Discrete-Time Model for Triply Selective MIMO Rayleigh Fading Channels," *IEEE Trans. Wireless Commun.*, vol. 3, no. 5, pp. 1678-1688, Sept. 2004.